Micromechanics of fiber composites at elevated temperatures

Alexander Tesar

Rakenteiden Mekaniikka, Vol. 35
Nro 2, 2002, s. 14-24

ABSTRACT

Numerical and experimental assessment of the ultimate behaviour of the fiber composites at elevated temperatures is treated in the present paper. The wave approach of the backpropagation neural network in micromechanical modeling, adopting the parallel processing FETM scheme, is used in the numerical analysis of the problem. Some numerical and experimental results obtained are submitted in order to demonstrate the efficiency of the procedures suggested.

INTRODUCTION

Numerical and experimental research of the ultimate behaviour of fiber composites at elevated temperatures has recently become the focus of intense efforts because of pressing problems of disaster prevention of modern structures made of such materials,
as are cable-stayed bridges, space facilities, guyed masts, cable roofs, lines of high voltage air conductors, etc. Required is sophisticated analysis in order to answer the questions associated with ultimate behaviour and reliability of such structures often acting in heavy exploiting and forcing conditions.

For the assessment of structures made of conventional materials, such as steel, wood or concrete, a lot of standards are available. For the structures made of the glass or carbon fiber composites the standards are rare and engineers are facing high requirements for their analysis.

The fiber composites adopted nowadays in structural engineering are made of three typical components listed as:

1. E-glass fibers made of calcium and aluminium boro-silicate composition and S-glass fibers made of magnesium and aluminium silicate composition having strength and elasticity moduli in scope 1.7 – 4.8 and 70 – 90 GPa, respectively,
2. carbon fibers with strength and elasticity moduli in scope 2.2 – 5.7 and 300 – 700 GPa, respectively,
3. aramide fibers with strength 3.5 GPa and elasticity moduli in scope 80 – 185 GPa.

The fiber composites consist of micromechanical fibers and surface resin skin. The calculation on the micromechanical level takes into account the behaviour of the single fiber in interaction with another fibers as well as with the surface resin skin.

For analysis is adopted the simulation model with wave analysis on the micromechanical level considering the behaviour of multi-string elements configurated in neural network mesh adopted.

In this paper the following is presented

1. the mathematical formulation of the governing wave equations for the ultimate analysis of the fiber composites at elevated temperatures,
2. brief description of the numerical treatment of the ultimate analysis at elevated temperatures,
3. numerical and experimental verifications.

WAVE APPROACH

When a fiber composite contains densely packed inclusions, the interaction effects of inclusions may play a dominant role in the ultimate behaviour of the resulting continuum at elevated temperatures. The concept of transformation strain can be used when an elastic medium contains periodically distributed inclusions or voids in material. Because of the periodicity, the transformation strains as well as other field quantities entering in the estimate of elastic moduli are periodic functions of space, time and temperature. The periodicity is exploited in an effort to obtain accurate estimates for the transformation strains which are used to approximate mechanical properties of the composites studied.

The Washizu´s variational principle is adopted below in order to include initial stress and strain components due to isothermal deformation at the same time. The stress in the microelement at the beginning of time and temperature increments studied is considered as initial stress with thermal strain increments. The variational principle under consideration is then written in the terms of time rate quantities given by

$$I = \{\int_V [S_{ij}\,\varepsilon_{ij} + 0.5\,W_{ij}\,u_{ki}\,u_{kj} - (\varepsilon^{\circ}_{ij} + 0.5\,\varepsilon'_{ij})\,S_{ij}]\,dV - \int_{A1} r_i^{(\cdot)}\,u_i\,dA1 - \int_{A2} s_i\,(u_i - w_i)\,dA2\}(dt)^2$$

$$+ \{\int_V W_{ij}\,\varepsilon_{ij}\,dV - \int_{A1} r_i\,u_i\,dA1 - \int_{A2} p_i\,(u_i - w_i)\,dA2\}dt \quad , \quad (1)$$

where W_{ij} and S_{ij} are the Piola-Kirchhoff stress tensors for initial stress and strain rate states, respectively, p_i and s_i are the Lagrangian surface traction and its time rate quantity, respectively, r_i and $r_i^{(.)}$ are prescribed on surface area A1 and w_i on area A2 and V is the volume bounded by surface area A=A1+A2. The total strain rate ε_{ij} is composed of the initial strain rate $\varepsilon^{o}ij$ and ε'_{ij}, corresponding to the instantaneous stress rate S_{ij} . To evaluate the thermal strain rate the thermal expansion coefficient at temperature T be $\alpha(T)$ and at temperature T+dT is given by $\alpha(T+dT)$. By expanding $\alpha(T+dT)$ into Taylor series, the average thermal strain rate is obtained.

The governing wave equation for the treatment of the ultimate behaviour is given by

$$\mu\,\eta(u_t) + (\lambda + \mu)\,\mathrm{grad}(\mathrm{div}\,u_t) + f = \rho\,\partial^2 u_t/\partial t^2 \quad , \quad (2)$$

where λ and μ are Lame´s constants, mass density is ρ, corresponding Laplace operator is η, the body force vector is f and the vector of displacements is u_t (Tesar and Svolik 1993).

In the terms of derivatives of displacement components u_t the governing wave equation is modified by

$$c_2\,u_t + (c_1^{\,2} - c_2^{\,2})\,u_t + f_i/\rho = a_t \quad , \quad (3)$$

with propagation velocities for dilatational waves

$$c_1 = \sqrt{[(\lambda + 2\mu)/\rho]} \quad , \quad (4)$$

and shear waves

$$c_2 = \sqrt{(\mu/\rho)} \quad . \quad (5)$$

Strain and stress components are defined by

$$\varepsilon_{ij} = (u_{i,j} + u_{j,i})/2 \qquad (6)$$

and

$$\sigma_{ij} = \lambda\,\varepsilon_{kk}\,\delta_{ij} + 2\,\mu\,\varepsilon_{ij} \quad , \; i,j = 1, 2, 3, \qquad (7)$$

with the Kronecker delta function δ_{ij} .

PARALLEL PROCESSING

Mathematical and physical backgrounds of the micromechanical simulation based on the idea of parallel processing as a part of neural network approach suggested are described below.

Assumed is the Euclidean n-dimensional space B^n. An open interval (a,b) is stated in B^1 assuming $a<b$ and $a,b \in B^1$. The symbol $G^{(k)}(a,b)$, with $k \in N$, is a set of real functions with continuous derivatives of the order $s(0 \leq s \leq k)$ in (a,b). $C^{(k)}(<a,b>)$ is the set of the functions from $C^{(k)}(a,b)$, with derivatives continuously expanded into <a,b>. $L(B^n)$ is the set of real matrices n x n.

Let in <a,b> be assumed the system of n-linear differential equations of the first order, given by

$$u_i'(t) = \sum a_{ij}(t)\, u_j \quad , \quad i = 1, 2, \ldots n \quad , \quad (8)$$

where $a_{ij}(t) \in C^{(o)}(<a,b>)$ holds for all i and j.

In the vector notation the system (8) is given by

$$u' = A\, u \quad . \quad (9)$$

Definition 1. An n-dimensional column vector $u(t) = [(u_j(t))^n_{j=1}]^T$ is the solution of the system (9) if

$$\forall_j: \quad u_j(t) \in G^{(1)}(<a,b>) \quad , \quad (10)$$

$$\forall t \in <a,b> : \quad u' = A\, u \quad . \quad (11)$$

Theorem 1. The solutions of the system (9) create the n-dimensional vector space in the field of real numbers. The matrix having n-columns and containing all fundamental solutions of the system (9) is denoted by $\Phi(t)$.

Theorem 2. The necessary and sufficient condition for the validity of the matrix $\Phi(t)$ for the solutions $(\{\Phi_i(t)\}_1^n$ is $\det \Phi(t)\, G$, where G is the constant regular matrix of the same type.

Definition 2. An n x n square matrix of type

$$U_A(a,t) = \Phi(t)\, \Phi^{-1}(a) \quad , \quad \forall t \in <a,b> \quad , \quad (12)$$

holds in the interval <a,t>.

The simulation model for the ultimate behaviour at elevated temperatures is established using the string mesh as shown in Fig. 1. For physical interpretation of the above definitions the in-
ternal and left-hand external wave displacements of one spring microelement as shown in Fig. 2 are denoted by u_a and u_b. The u_a will match the u_b when the microelement is moved one bay to the right, so that u_a and u_b share the same dimension. The internal wave displacement vector u_i is eliminated beforehand, giving the stiffness matrix by

$$K(\omega) = \begin{bmatrix} K_{aa} & K_{ab} \\ K_{ba} & K_{bb} \end{bmatrix} \quad , \quad (13)$$

and the displacement wave vector by

$$u = \begin{bmatrix} u_a \\ u_b \end{bmatrix} \quad . \quad (14)$$

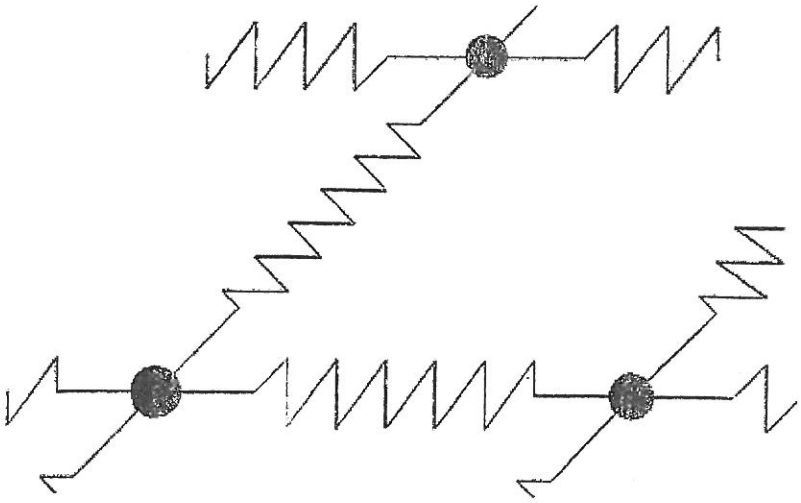

Fig. 1. Spring microelement simulation model adopted

The coreresponding force vectors are given by

$$n_a = K_{aa}\, u_a + K_{ab}\, u_b \quad , \quad (15)$$

$$n_b = -K_{ba}\, u_a - K_{bb}\, u_b \quad . \quad (16)$$

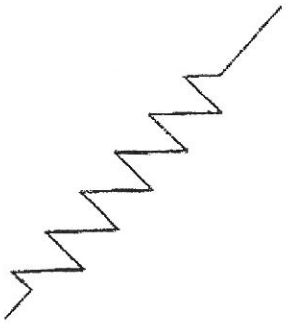

Fig. 2. Single spring element

The state wave vector v is defined as the combination of wave displacements and wave internal forces given by

$$v = [u, n]^T \quad . \quad (17)$$

The the wave state vector at boundaries a and b is given by

$$v_b = S\, v_a \quad , \quad (18)$$

with corresponding wave transfer matrix S. It holds

$$S = \begin{bmatrix} S_{aa} & S_{ab} \\ S_{ba} & S_{bb} \end{bmatrix} , \quad (19)$$

with

$$S_{aa} = -K_{ab}^{-1} K_{aa} \quad , \quad S_{ab} = K_{ab}^{-1} \quad , \quad S_{ba} = -K_{ba} + K_{bb} K_{ab}^{-1} K_{aa} \quad , \quad S_{bb} = -K_{bb} K_{ab}^{-1} \quad . \quad (20)$$

The damping parameters are contained in complex elasticity moduli appearing in stiffness terms of the corresponding wave transfer matrix S.

The calculation run of the FETM wave approach is adopted below with updated variability of the multibody simulation mesh size in space and time. The details of the parallel processing FETM wave approach are summed up, for example, in Tesar and Fillo 1988 or in Tesar and Svolik 1993.

NEURAL NETWORK

Neural network has been developed recently for the solution of some sophisticated problems in structural engineering. Comparing to the conventional digital computing techniques the neural networks are advantageous because of their special features such as parallel processing, distributed storing information, low sensitivity of error, very robust in operation after training and adaptability to new information.
The idea for application of the neural network in structural engineering appeared in Adeli and Yeh 1989. After that neural networks have been used in the areas such as structural analysis and design, material behaviour and damage identification. Among these applications the neural network trained by backpropagation algorithm is the most utilized neural network primarily due to its simplicity.

The topology of the backpropagation neural network adopted (Wei Lu and Mäkeläinen, P. 2001) and the training algorithm are described briefly below. It is a multilayered feedforward neural network trained by backpropagation algorithm. The topology of the neural network is plotted in Fig. 3, including the input layer, one or several hidden layers and the output layer. The fundamental building block of the neural network is called artificial node and is shown in Fig. 4. The node is composed of a set of connecting spring links characterized by their own weight, of an adder used to sum the weighted input, of an activation function used to decrease the magnitude of the output and of a threshold of the activation function.

The backpropagation algorithm starts with randomly initialized weights. Using the calculation rule for one node, the input vector is feedforwarded from layer to layer until the output is produced.

The calculation rule for one basic node of the backpropagation neural network adopted is given by

$$y = f(net) = f(\Sigma w_i x_i - \Theta) \quad , \quad (21)$$

where x_i is the i-th component of the input vector, w_i is the i-th component of the weight vector, Θ is the threshold, f is the activation function, y is the output of the node and t_i is the i-th component of the target vector which is the desired output of the neural network corresponding to the input vector.

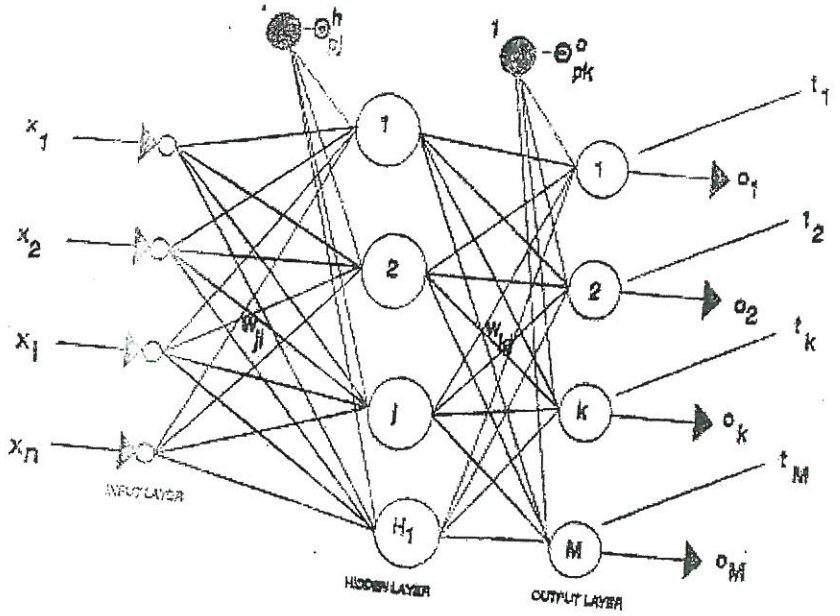

Fig. 3. Topology of the backpropagation neural network

The backpropagation algorithm starts with randomly initialized values. Using the calculation rule for one node the input vector is feedforwarded from layer to layer until the output is produced. The output vector is compared with target vector and the error in the output layer is calculated using

$$\delta_{pk} = (t_{pk} - o_{pk})\, f_k\, (1 - f_k) \quad , \quad (22)$$

where t_{pk} and o_{pk} represent target and output values of the k-th node in the output layer corresponding to the p-th training pattern and f_k is the activation function for the k-th node.

Adopting the above approach, the calculation run of the ultimate fatigue analysis is given by following operations:

1. Micromechanical modeling of the material and structural configurations in space, time and temperature.
2. Updated calculation of the wave stress and strain states in space, time and temperature adopting the above backpropagation neural networks approach.
3. Automatic comparison with ultimate strength of the micromechanical elements of the model used.
4. Initiation of the cracks in micromechanical elements trespassing the ultimate strength.

5. Updated calculation of the crack growth with the development of the cracks in space, time and temperature until total destruction of the specimen studied.

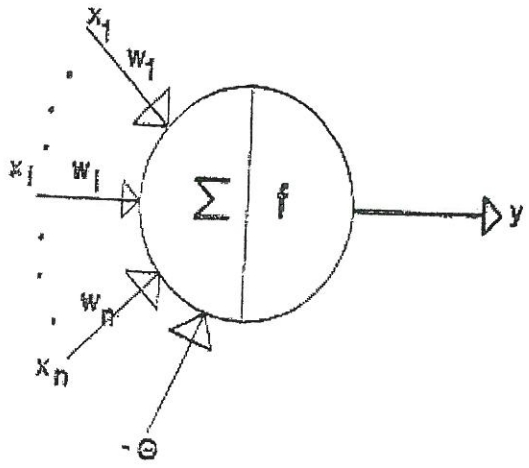

Fig. 4. Artificial node

The regime of the crack initiation and growth is rather complex. One or several cracks develop and propagate slowly along the critical regions of the specimen studied. In the case of the shear loading the cracks usually turn inside of the body in a direction that is quasi-perpendicular to the tension.

NUMERICAL AND EXPERIMENTAL ASSESSMENT

Above theoretical approaches were adopted in ramification of the research or the standard tension specimens with thickness 3 mm as shown in Fig. 5, made of the fiber glass composite EXTREN and subjected to the tension at elevated temperatures.

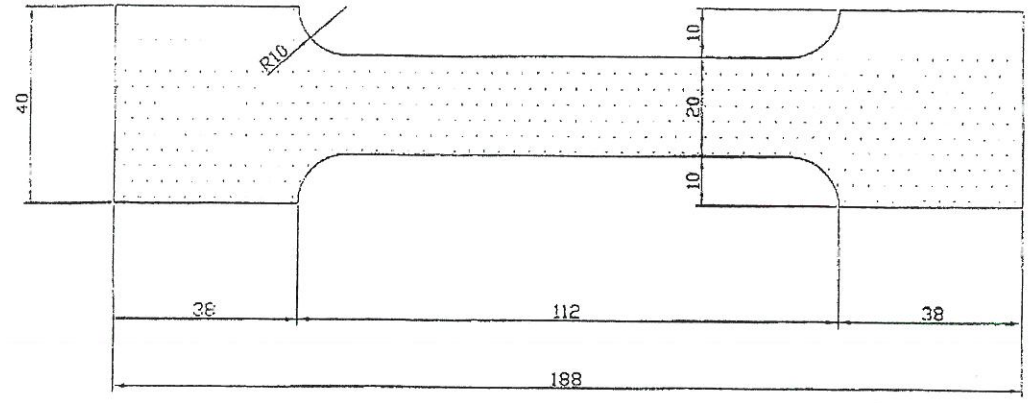

Fig. 5. Standard glass fiber specimen studied

Special laboratory equipment was adopted for thermal testing of the specimens studied. The temperature development was initiated via electrical resistance wires attached midspan of the specimens tested. Two series of laboratory tests were made at elevated temperatures and tension forces adopted.

The first series Nr. (357 T) consisted of five tests performed under the simultaneous action of tensile forces 3, 5 and 7 kN (357) and temperature 0, 26, 51, 82 and 119° C (T). The numerical and experimental results obtained are summed up in Table 1. The second series consisted of two tests performed under the simultaneous action of tensile forces 3, 6 and 9 kN and temperature 0 and 22° C. The numerical and experimental results obtained are summed up in Table 2.

Table 1. Stress, strain and elasticity moduli under the action of tensile force and temperature in the first test series

Specimen Nr.	357 000	357 026	357 051	357 082	357 119
Temperature [°C]	0	26	51	82	119
Max. force [kN]	6.983	6.012	6.983	6:871	6.946*
Max. stress [MPa] – calculated	116.451	115.468	116.450	114.542	82.653
measured	116.383	115.200	116.383	114.517	82.433
Plastic strain [promile] - calculated	0.25	0.25	0.37	0.40	0.50
measured	0.25	0.25	0.37	0.40	0.50
Max. strain [promile] - calculated	4.292	4.498	4.912	5.431	4.301
measured	4.273	4.471	4.802	5.245	4.137

Elasticity modulus [GPa] – calculated	27.263	25.921	24.497	21.993	19.948
measured	27.237	25.766	24.236	21.834	19.926

*Maximal force obtained in the specimen

CONCLUSIONS

Theoretical approach and numerical as well as experimental results sampled up in the present paper submit some image on the ultimate response of the fiber composites at elevated temperatures. The micromechanical wave approach and the numerical analysis performed are based on the updated discrete simulation of the problem in space, time and temperature. Experimental verifications confirmed the coincidency with theoretical and numerical approaches performed.

ACKNOWLEDGEMENTS

The author would like to aknowledge the grant agency VEGA (Ministry of Education, Slovak Republic) for the initiation and supporting of above research project.

Table 2. Stress, strain and elasticity moduli under the action of tensile force and temperature in the second test series

Specimen Nr.	369 002	369 022
Temperature [°C]	2	22
Max. force [kN] – calculated (measured)	8.943 (8.939)	8.882 (8.868)
Max. stress [MPa] – calculated (measured)	149.012 (148.983)	147.989 (147.800)
Plastic strain [promile] – calculated (measured)	0.52 (0.50)	0.82 (0.80)
Max. strain [promile] – calculated (measured)	5.012 (5.009)	5.379 (5.353)
Elasticity modulus [GPa] – calculated (measured)	29.751 (29.743)	27.628 (27.611)

REFERENCES

[1] Tesar, A., Fillo, L.: Transfer Matrix Method, KLUWER Academic Publishers, Dordrecht/Boston/London, 1988

[2] Tesar, A. and Svolik, J,: Wave distribution in fibre members subjected to kinematic forcing. Int. Journal for Communication in Numerical Mechanics, 9, 1993

[3] Simo, J.C.: On a fully three-dimensional finite strain viscoelastic damage model – formu-lation and computational aspects. Comput. Meth. Engng. 29, 1990

[4] Adeli, H. and Yeh, C.: Perception Learning in Engineering Design. Microcomputers in Civil Engineering, 4, 1989

[5] Lu, W. and Mäkeläinen, P.: A neural network model for local and distortional buckling behaviour of cold-formed steel compression members. Proceedings of 9-th Nordic Steel Construction Conference, Helsinki, 2001

[6] Duk-Hyun Kim: Composite Structures for Civil and Architectural Engineering, South Korea, 1995
[7] Extren Design Manual, Strongwell Corporation 1998, Bristol, Virginia
[8] Tesar, A. and Simoncic, M.: Fatigue analysis of fiber glass composites. Building Research Journal, 2, 2002
[9] Tesar, A., Sotakova, D. and Minar, M.: Micromechanics of fiber glass composites at elevated temperatures. Int. Journal for Numerical Methods in Engineering, 4, 2002

Alexander Tesar
Civ.Eng., PhD, DrSc, Prof.
Institute of Construction and Architecture
Slovak Academy of Sciences
Dubravska cesta 9
842 20 Bratislava
SLOVAK REPUBLIC
E-mail: usarate@savba.sk